First-principles study of substitutional carbon pair and Stone–Wales defect complexes in boron nitride nanotubes

Gunn Kim [*],[1], Jinwoo Park [1], Suklyun Hong [*]

Department of Physics, Graphene Research Institute and Institute of Fundamental Physics, Sejong University, Seoul 143-747, Republic of Korea

ARTICLE INFO

ABSTRACT

Using density functional theory, we study physical properties of boron nitride nanotubes (BNNTs) with the substitutional carbon pair defect. We also consider the Stone–Wales (SW) rearrangement of the C–C pair defect in the BNNT. The formation energy of an SW defect of the carbon dimer is approximately 3.1 eV lower than that of the SW-transformed B–N pair in the undoped BNNT. The activation energies show that the SW defect in the C-doped BNNT may be experimentally observed with a higher probability than in the undoped BNNT. Finally, we discuss the localized states originating from the carbon pair impurities.

© 2011 Elsevier B.V. All rights reserved.

1. Introduction

As a wide-band-gap nanomaterial [1–3], hexagonal boron nitride (h-BN) is a stable crystalline form consisting of equal numbers of boron and nitrogen atoms in a honeycomb arrangement [4–6]. As it has considerably high thermal and chemical stabilities [7], it can be used for high-temperature applications. The BN nanotube (BNNT) [8,9] is a nano-sized seamless cylinder that can be considered a rolled-up h-BN sheet. It also has a wide band gap that is almost independent of the tube diameter, and chirality [10]. For sp^2-bonded carbon nanostructures such as fullerenes, carbon nanotubes and graphene, the Stone–Wales (SW) transformation [11] is believed to introduce topological defects or isomerization, which results in a 90° rotation of two carbon atoms with respect to the midpoint of the C–C bond.

When an SW defect is present in h-BN or BNNT, B–B and N–N bonds should be created, and the formation of these bonds increases the total energy of the system. Thus, the topological defect created by the SW rearrangement is lacking. However, the formation of B–B and N–N bond pairs can be avoided if there is a C–C pair defect in h-BN (or BNNT). Using post-synthesis doping, carbon impurities can be substituted in the h-BN layers [12–14]. During the formation of BNNTs and h-BN sheets using the chemical vapor deposition (CVD), carbon atoms may act as substitutional defects, because residual hydrocarbon may remain in the chamber, or carbon impurities are solubilized in the metal catalyst. If carbon substitutional atoms congregate together in a local area in h-BN

(or a bundle of BNNTs) by segregation, they may form the interlayer (or intertube) conduction channels. As mentioned above, the C–C pair defect in the h-BN network prohibits the formation of B–B and N–N bonds during the SW transformation. As the SW-transformed defects may affect the mechanical and electrical properties of the BN nanostructures, we should thus study these defects in the C-doped BN sheets or BNNTs. This work may explain the formation of topological defects in the carbon-doped BNNTs or h-BN layers that can be produced in the CVD processes. In this Letter, we present our first-principles study of the structural and electronic properties of the BNNTs containing two substitutional carbon defects. The effect of carbon doping on the SW transformation is also examined.

2. Computational details

We carried out total energy calculations for our model systems based on the density functional theory [15]. The local density approximation (LDA) [16] with spin polarization was used for the exchange–correlation functional. To study the energetics and the activation energy barrier in the SW transformation of the systems, we used a plane wave basis set with an energy cutoff of 400 eV and ultrasoft pseudopotentials [17] implemented in the Vienna ab initio simulation package (VASP) [18,19]. The atomistic models were relaxed until the residual forces on the atoms became smaller than 0.03 eV/Å. For the activation energy barrier, we employed the nudged elastic band method [20]. Eight replicas were selected, including the initial and final configurations to construct an elastic band. To plot the density of states (DOS) and the wavefunctions with phase information, we used the OpenMX code [21]. In the calculations using the OpenMX code, the ionic potentials were described with norm-conserving Troullier–Martins pseudopoten-

* Corresponding authors. Fax: +82 2 3408 4316.
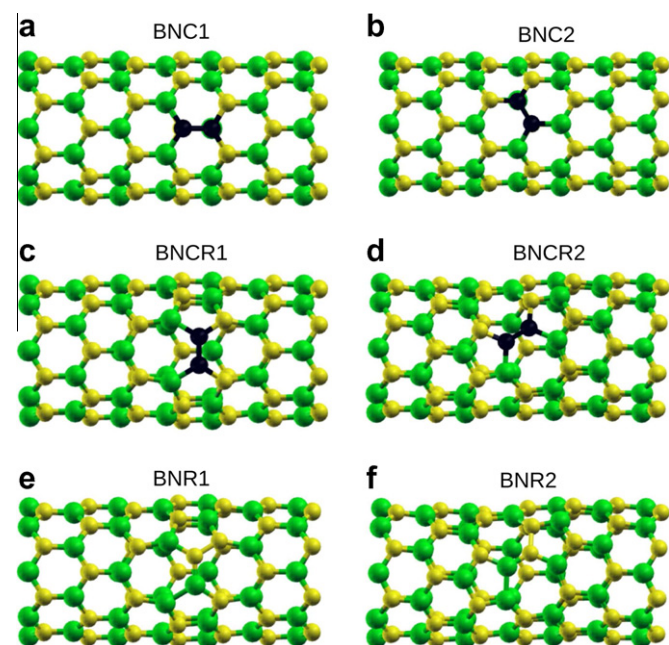E-mail addresses: gunnkim@sejong.ac.kr (G. Kim), hong@sejong.ac.kr (S. Hong).
[1] These authors contributed equally to this work.

tials. Wavefunctions were expanded in a pseudoatomic orbital basis set [22] with an energy cutoff of 120 Ry. As a model system, we chose the (8,0) zigzag BNNT containing 48 B atoms and 48 N atoms. The supercell size in the lateral direction was 25 Å to avoid the interaction between the defects in neighboring BNNTs, and the size in the axial direction was 12.96 Å.

3. Results and discussion

First, we optimized the C-doped and undoped BNNTs. The perfect BNNT has a B–N bond length of ∼1.44 Å. Our total energy calculations show that the two substitutional carbon atoms tend to bind to each other. This finding agrees with Yuge's report that the lowest-formation-energy structures for monolayer boron–carbon-nitride favor B–N and C–C bonds whereas they disfavor B–C, C–N, B–B, and N–N bonds [23]. For C-doping, two types of C–C pairs can be considered. As shown in Figure 1, one pair (BNC1) was parallel to the tube axis and the other (BNC2) had an oblique angle with the tube axis. The bond length of the C–C pair was 1.37 Å (1.39 Å) for BNC1 (BNC2). The bond length of benzene (C$_6$H$_6$) has a very similar C–C bond length of 1.40 Å. Although the model of BNC1 had the lowest energy among our model systems for the C–C pair, the energy difference between BNC1 and BNC2 was only ∼1 meV/atom. Thus, two structures may coexist. In fact, by the chemical potential analysis we find that the formation of carbon substitutional defects in the BNNTs, BNC1 or BNC2, is possible when the chemical potential of an isolated C–C pair is larger than by −18.02 eV or −17.90 eV. Note that the energy of an C–C pair is −10.09 eV.

In the C–C pair, the C atom bonded to two B atoms protruded out by ∼0.1 Å. The B–C bond length was 1.52 Å and the N–C bond length was 1.46 Å, which was due to the longer covalent radius of B ($r_{covalent,B}$ = 0.84 Å) than that of N ($r_{covalent,N}$ = 0.71 Å). When

the C–C bond was rotated by 90°, the bond length slightly decreased to 1.35 Å. Here, the B–C bond length was increased to 1.61 Å, and the N–C bond length was slightly decreased to 1.44 Å. After the SW transformation from the BNC1 to the BNCR1 structure, the total energy of BNCR1 increased by 2.5 eV, compared to that of BNC1. For this structure, the activation energy from BNC1 to BNCR1 was 5.5 eV. Similarly, the formation and activation energies were 2.2 and 5.6 eV, respectively, for the SW transformation from BNC2 to BNCR2 (see Table 1).

For comparison, we also calculated the formation and activation energies for the SW transformation in the undoped (8,0) BNNT as shown in Figure 2. For the SW transformation from BN1 to BNR1 (or from BN2 to BNR2), the formation energy was 5.6 eV (5.7 eV), and the activation energy was 7.0 eV (7.6 eV). Here, a B–B bond and a N–N bond are produced, and their lengths are 1.73 Å(B–B) and 1.47 Å(N–N), respectively. We found that the rotating C–C bond (1.24 Å) was shorter than the rotating B–N bond (1.29 Å) in the transition states. This implies that the shorter bond results in a lower activation energy barrier during the SW transformation in a small area. The high formation energy is due to the unstable B–B and N–N bonds as mentioned earlier. Interestingly, electrons were accumulated in the N atom of the rotating B–N pair in the transition state for the undoped BNNT. In addition, our charge analysis revealed that electron donation from the C–C pair defect in the C-doped BNNT slightly weakens the dangling-bond-like character of the B and N atoms in the transition configuration. In our previous study of the SW transformation in M@C$_{60}$ (M = K, Ca, and La), we similarly observed that the electron donation by the incorporated metal atom lowers the activation energy barrier [24]. These findings can explain the lower activation energy barrier of the C–C pair defect compared to that of the B–N pair. Therefore, when the C-doped BNNT *does* exist, e.g., from the sample preparation, we can conclude that the probability that the SW defect is observed is higher in the C-doped BNNT than in the undoped BNNT.

Some total-energy calculations were repeated using the generalized gradient approximation. We found that the exchange–correlation functional did not change our main conclusion that the SW defect in the C-doped BNNT may be observed with a higher probability than in the undoped BNNT.

To check a charge doping effect, we calculated doping of a hole (charge +e state) for all the model structures (BNR1, BNR2, BNCR1, and BNCR2), and an electron doping case (charge −e state) for BNR2 structure. When a hole was doped, the activation energy barriers were *reduced* from 7.04 to 6.91 eV for BNR1, 7.63 to 7.18 eV for BNR2, 5.50 to 5.23 eV for BNCR1, and 5.64 to 5.52 eV for BNCR2, respectively. For an electron doping in BNR2, the activation energy was *decreased* from 7.63 to 6.69 eV. Therefore, we can conclude that charge doping affects the activation energy barriers of the SW transformation.

In a growth process of the BNNTs, carbon atoms may be incorporated as residual impurities. Or one can produce carbon substitutional defects in the BNNTs on purpose for doping. Our results demonstrate that two carbon atoms far from each other tend to become closer and form a C–C pair. The energy difference between the C–C pair and two separate carbon atoms was larger than 5 eV in our LDA calculation. On the other hand, some metal atoms or

Figure 1. Optimized structures of (8,0) BNNTs with a C–C pair substitutional defect or the SW defects. (a) The BNNT with a C–C pair substitutional defect parallel to the tube axis, (b) the BNNT with a C–C pair substitutional defect with an oblique angle with respect to the tube axis. (c) and (d) Show the SW-transformed C–C pair defect from (a) and (b), respectively. (e) and (f) Are the BNNTs with SW defects which are parallel and tilted to the tube axis, respectively. Yellow, green and black balls represent nitrogen, boron and carbon atoms, respectively. (For interpretation of the references to color in this figure legend, the reader is referred to the web version of this article.)

Table 1
Calculated activation (E_a) and formation (E_r) energies for the SW transformation from the C-doped or the t BNNTs to the BNNTs with SW defects.

|	E_a (eV)	E_r (eV)
BNC1 → BNCR1	5.50	2.51
BNC2 → BNCR2	5.64	2.17
BN1 → BNR1	7.04	5.61
BN2 → BNR2	7.63	5.72
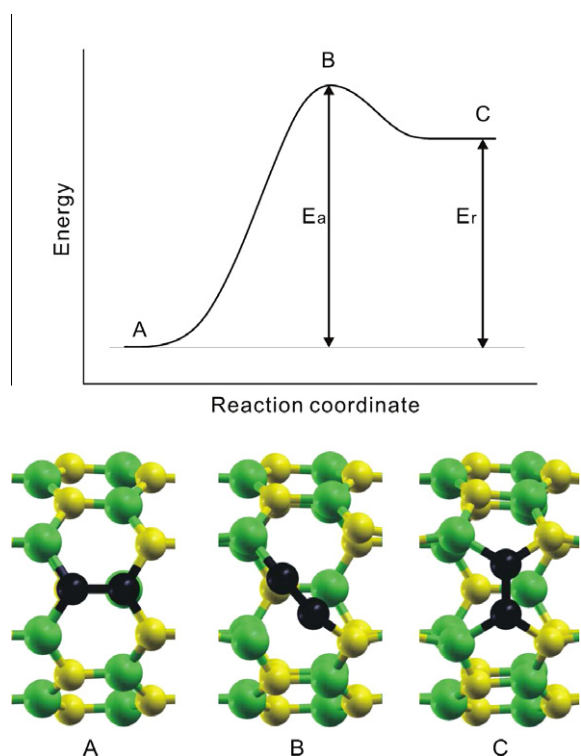
Figure 2. (Top panel) Energy profile along the reaction coordinate in the SW transformation of BNNTs with a C–C pair substitutional defect or the SW defects. The states "A", "B", and "C" represent the initial, transition, and final states in the SW transformations, respectively. The activation and formation energies are denoted as E_a and E_r, respectively. (Bottom panel) The corresponding three states are shown for the SW transformation from BNC1 to BNCR1.

Figure 3. (a) Total DOS of the perfect (8,0) BNNT. Total DOS of BNNTs with (b) the C–C pair substitutional defect or (d) the SW defects. Dotted lines in (c) and (e) indicate the projected DOS of two C atoms in the C–C pair defect in each case.

molecules such as O_2 and Br_2 may be adsorbed in the vicinity of the C–C pair. Then, electron transfer takes place between the adsorbate and the nanotube. As mentioned above, charge doping enables the activation energy barrier to become lowered and the probability of the SW transformation to become higher.

According to our LDA calculation, the energy band gap of the perfect (8,0) BNNT is 3.6 eV as shown in Figure 3a. Wu et al. reported that the BNNT could have a magnetic moment due to the carbon doping [25]. They considered only one carbon atom in the supercell. However, our calculational results demonstrated that the magnetic moment does not occur in the BNNT with the C–C pair defect. According to a recent report by Berseneva et al., the magnetic moment is zero when the numbers of carbon atoms replaced by nitrogen and boron atoms are identical [26]. Figure 3b shows the total DOS of BNNTs with the C–C pair substitutional defect (e.g., BNC1), which clearly demonstrates that a few localized states occur in the band gap in the presence of the C–C pair defect. As shown in Figure 3c, the projected DOS of the two C atoms in the C–C pair defect indicates that the gap states originate from the substitutional carbon pair defects. When a C–C pair forms a SW defect by a 90° rotation as seen in BNCR1, the electronic states originating from the SW defect have flatter bands with more localized characters. These characteristics are reflected in the sharp and narrow peaks in the DOS in the gap (Figure 3d and e).

Figure 4 shows wavefunction characters resulting from the defect states in the BNNTs with the substitutional carbon pair defect and its SW-transformed defect. The occupied state at −1.4 eV and the unoccupied state at +1.7 eV shown in Figure 4a are the localized defect states originating primarily from the C–C pair of the BNC1 structure. The filled state has a bonding character, whereas the unfilled state has an antibonding character at the C–C
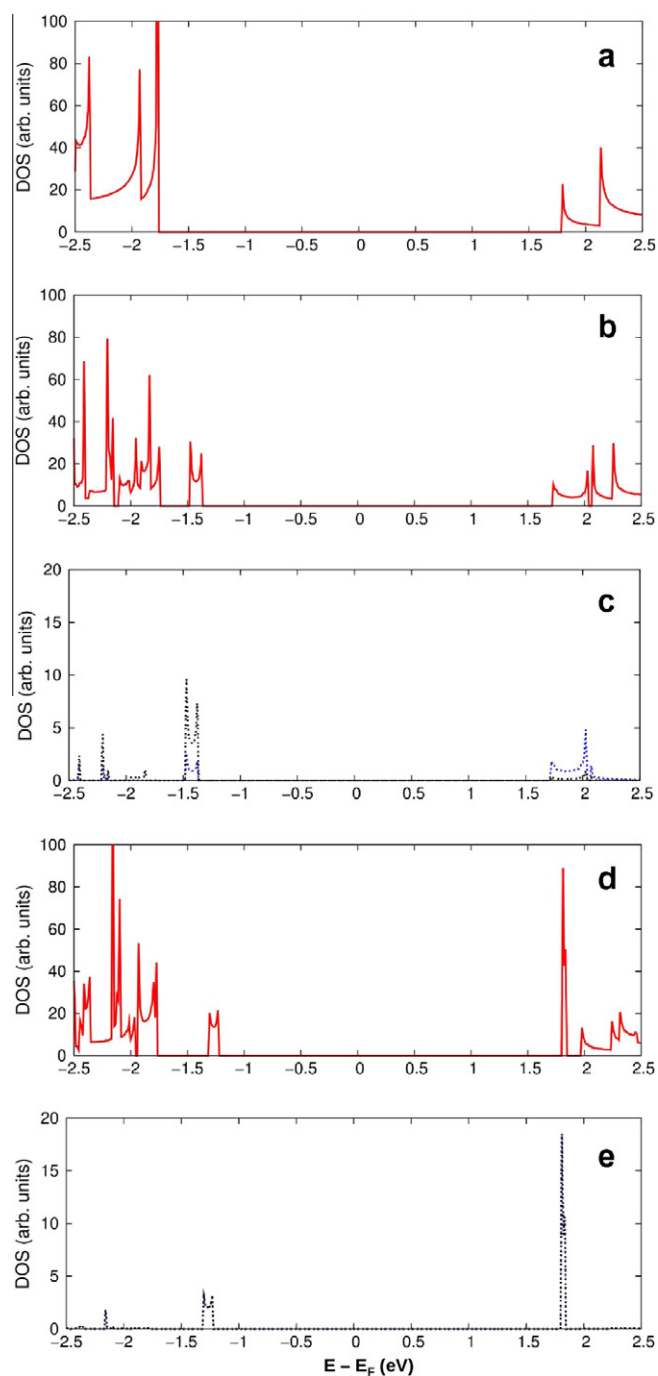
pair. As displayed in Figure 4a, the electron density at the C atom bonded to B atoms is somewhat higher than that at the C atom bonded to N atoms at −1.4 eV. Additionally, the B–C bonds are in the bonding states but the C–N bonds are in the antibonding states. On the other hand, Figure 4b shows the localized defect states at −1.3 eV and +1.8 eV from the SW-transformed C–C pair defect of the BNCR1 structure. Similar to the BNC1 case, bonding and antibonding characters of the carbon pair appear at −1.3 eV and +1.8 eV, respectively. Note that there is no mirror (reflection) symmetry for the BNNT with respect to the plane containing the midpoint of the C–C bond. However, the mirror symmetry is
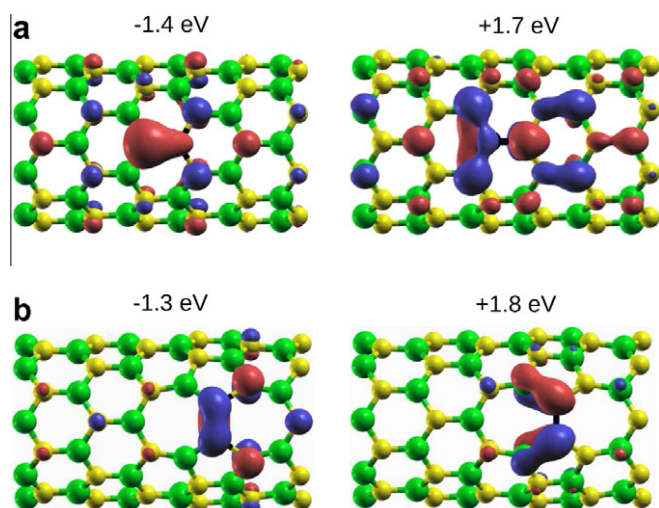
Figure 4. Wavefunctions originating from the defect states in the BNNTs with (a) the substitutional C–C pair defect (BNC1) and (b) the SW-transformed C–C pair defect (BNCR1). Red and blue colors represent the opposite signs in the wavefunctions at the Γ-point. (For interpretation of the references to color in this figure legend, the reader is referred to the web version of this article.)

manifest with respect to the planes containing the C–C bond itself (as in BNC1) as well as the midpoint of the SW-transformed C–C bond (as in BNCR1). These features were retained for two localized states as shown in Figure 4a and also for a localized state at −1.3 eV as shown in Figure 4b.

4. Conclusion

In summary, we have introduced substitutional carbon pair defects in BNNTs to examine the modifications in the structural and electronic properties of the nanotube. Our results demonstrate that the two carbon atoms prefer to bind to each other with a bond length of ~1.37 Å. For the SW transformation of the C–C pair defect, the formation energy of the SW defect is approximately 2.5 eV and the activation energy is approximately 5.5 eV. Both the formation and activation energies of the C–C bond are much lower than those of the B–N bond in the undoped BNNT in the SW transformation, which are ~5.5 and ~7.0 eV, respectively. Consequently, it would be very difficult to find a topological defect such as the SW defect in the perfect BNNT. Conversely, such a topological defect could be observed with a higher probability in the C-rich defective BNNTs.

References

[1] Y.N. Xu, W.Y. Ching, Phys. Rev. B 44 (1991) 7787.
[2] M.S. Si, D.S. Xue, Phys. Rev. B 75 (2007) 193409.
[3] X. Blase, A. Rubio, S.G. Louie, M.L. Cohen, Europhys. Lett. 28 (1994) 335.
[4] K. Watanabe, T. Taniguchi, H. Kanda, Nat. Mater. 3 (2004) 404.
[5] A. Rubio, J.L. Corkill, M.L. Cohen, Phys. Rev. B 49 (1994) 5081.
[6] N.G. Chopra, R.J. Luyken, K. Cherrey, V.H. Crespi, M.L. Cohen, S.G. Louiea, A. Zettl, Science 269 (1995) 966.
[7] D. Golberg, Y. Bando, C.C. Tang, C.Y. Zhi, Adv. Mater. 19 (2007) 2413.
[8] A. Loiseau, F. Willaime, N. Demoncy, G. Hug, H. Pascard, Phys. Rev. Lett. 76 (1996) 4737.
[9] D. Golberg, Y. Bando, W. Han, K. Kurashima, T. Sato, Chem. Phys. Lett. 308 (1999) 337.
[10] G.G. Fuentes, E. Borowiak-Palen, T. Pichler, X. Liu, A. Graff, G. Behr, R.J. Kalenczuk, M. Knupfer, J. Fink, Phys. Rev. B 67 (2003) 035429.
[11] A.J. Stone, D.J. Wales, Chem. Phys. Lett. 128 (1986) 501.
[12] O.L. Krivanek et al., Nature (London) 464 (2010) 571.
[13] X. Wei, M. Wang, Y. Bando, D. Golberg, J. Am. Chem. Soc. 132 (2010) 13592.
[14] X. Wei, M. Wang, Y. Bando, D. Golberg, ACS Nano 5 (2011) 2916.
[15] P. Hohenberg, W. Kohn, Phys. Rev. 136 (1964) B864.
[16] W. Kohn, L.J. Sham, Phys. Rev. 140 (1965) A1133.
[17] D. Vanderbilt, Phys. Rev. B 41 (1990) 7892.
[18] G. Kresse, J. Hafner, Phys. Rev. B 47 (1993) R558.
[19] G. Kresse, J. Furthmüller, Phys. Rev. B 54 (1996) 11169.
[20] G. Mills, H. Jónsson, Phys. Rev. Lett. 72 (1994) 1124.
[21] T. Ozaki, Phys. Rev. B. 64 (2001) 195110.
[22] T. Ozaki, Phys. Rev. B. 67 (2003) 155108.
[23] K. Yuge, Phys. Rev. B 79 (2009) 144109.
[24] W.I. Choi, G. Kim, S. Han, J. Ihm, Phys. Rev. B 73 (2006) 113406.
[25] R.Q. Wu, L. Liu, G.W. Peng, Y.P. Feng, Appl. Phys. Lett. 86 (2005) 122510.
[26] N. Berseneva, A.V. Krasheninnikov, R.M. Nieminen, Phys. Rev. Lett. 107 (2011) 035501.